

PROCEEDINGS OF SPIE

SPIDigitalLibrary.org/conference-proceedings-of-spie

All-fiber optical supercontinuum sources in 1.7-3.2 μm range

Vladislav V. Dvoyrin, Irina T. Sorokina

Vladislav V. Dvoyrin, Irina T. Sorokina, "All-fiber optical supercontinuum sources in 1.7-3.2 μm range," Proc. SPIE 8961, Fiber Lasers XI: Technology, Systems, and Applications, 89611C (7 March 2014); doi: 10.1117/12.2040785

SPIE.

Event: SPIE LASE, 2014, San Francisco, California, United States

All-Fiber Optical Supercontinuum Sources in 1.7-3.2 μm range

Vladislav V. Dvoyrin* and Irina T. Sorokina

Department of Physics, Norwegian University of Science and Technology, N-7491 Trondheim,
Norway

ABSTRACT

We report supercontinuum generation in the 1.7-2.9 μm range with up to 3.08 W of output power and in the range of 1.93-3.18 μm with up to 3.8 W of output power from all-fiber MOPA pulsed systems with Tm-doped fiber mode-locked seed laser. Supercontinuum generation was demonstrated in nonlinear germanate fibers and fluoride (ZBLAN) fibers. The supercontinuum bandwidth reached 1250 nm at -10 dB level.

Keywords: fiber optics, infrared, infrared and far-infrared lasers, femtosecond lasers, optical supercontinuum

INTRODUCTION

Optical supercontinuum (SC) sources in infrared spectral region are of great importance for a number of practical applications such as LIDAR systems¹, optical coherence tomography², chemical sensing and environmental monitoring³. For environmental science, the region of 2-3 μm is of particular interest, because of the absorption bands of important atmospheric constituents like CO₂ (2 and 2.7 μm) and trace gases and pollutants like CO (2.3 μm band), NH₄ (2.2-2.3 and 2.9 μm bands), CO (2.3-2.4 μm), N₂O (2.85-2.9 μm), CH₄ (2.4 μm), and others³. Recently, all-fiber lasers emitting in a broad region up to 2.8 μm were reported⁴⁻⁸, using a simple and practical setup based on silica Tm- and Ho-doped fiber MOPA lasers. Unfortunately, the emission intensity rapidly falls down at the wavelength exceeding 2.5 μm due to high optical loss in silica-based fibers. A number of other popular glass materials have been tested, e.g. fluoride, telluride and chalcogenide fibers^{5,9,10}, which have demonstrated very broad emission range, up to 7 μm ¹⁰. However, mechanical splices, low damage threshold, and possible surface degradation make such configurations questionable for a wide application in practice. In this paper we investigate a promising glass host – germanate fibers and compare their performance to a fluoride fiber. Germanate fibers utilize silica clad and germanium oxide-doped glass core (>50% GeO₂). Thanks to the silica clad, germanate fibers can be directly spliced with conventional silica-based fibers using commercial electrical fusion splicers. Such possibility together with their excellent stability and the resistance to the optical power load make them unique among other nonlinear fibers and attractive for practical applications. We show, that these oxide glass fibers allow to expanding the generated emission well beyond 3 μm , which is a key point for many applications related to sensing.

EXPERIMENTAL

We realized the all-fiber linear-cavity mode-locked seed laser based on a silica-based Tm-doped fiber and a SESAM semiconductor mirror⁸. The laser output was protected by an isolator. When pumped at the wavelength of 1560 nm by a diode laser, the laser produced an 2-ps pulse train at 44 MHz repetition rate and average power of 6.7 mW. The amplifier used a 4 m piece of a silica-based Tm-doped double-clad fiber with 10 and 130 μm core and first clad diameters, respectively, and 0.15 core numerical aperture. The amplifier was pumped by a fiber-coupled diode laser at 793 nm.

The amplifier output was spliced with nonlinear fibers based on fluoride glass (ZBLAN) or silica glass with a germanate glass core. The 2 m piece of the fluoride glass fiber with 9 μm core diameter and 0.17 numerical aperture was spliced mechanically; its ends were terminated with angle-polished connectors. For this purpose a piece of a standard telecom

fiber of 0.5 m length terminating with a compatible connector on one side was spliced to the laser output with an electrical fusion splicer. At 2 μm , the dispersion parameter for this fiber amounted to 7.5 ps/(nm \times km)⁹.

A set of 4 germanate fibers with cores with ~ 3 μm diameter and germanium content of about 50% was produced in FORC RAS, Moscow, Russia. The main difference between the fibers was their dispersion parameter at 2 μm equal to -15, -75 and -130 ps/(nm \times km) for the fibers 357, 343 and 311, respectively, and corresponding cut-off wavelength of 1.4, 1.4 and 1 μm , respectively. The last fiber from the set has a core of 9 μm diameter of pure GeO₂ glass. Its dispersion was not measured but from the theoretical estimations the clad weakly influenced the dispersive properties and the dispersion was assumed to be that of the bulk GeO₂ glass thus being negative (positive sign of the dispersion parameter) in contrast to the other investigated germanate fibers. The germanate fibers were spliced with electrical fusion splicer to a piece of a standard telecom fiber of 0.15 m length which was spliced to the laser output. The output ends were angle-cleaved.

Optical spectra were recorded with optical spectrum analyzer AQ 6375, Yokogawa Inc. (1.2-2.5 μm operation range) and Spectrum GX FTIR Spectrometer, PerkinElmer Inc. The pulse trains were observed with InGaAs semiconductor optical detector connected to a digital oscilloscope. The response time of the detector was about 1 ns.

RESULTS AND DISCUSSION

For all investigated laser configurations the output emission consisted of stable optical pulse trains with the repetition rate of the seed laser, 44 MHz. Due to Raman multi-soliton generation, output of the Tm-doped amplifier at high pump powers already had a bandwidth of about 550 nm at -10 dB level (Fig. 1a). The standard fiber terminated with a connector spliced to the amplifier inserted a noticeable optical loss of about 1 dB. The mechanical splice with the fluoride fiber provided further 2.15 dB loss, and that the output power from this fiber was only 2.3 W for 5 W of the amplifier output. The fiber transmission losses were negligible compared to the total splice losses. The output spectra at different output power levels are shown in Fig. 1b.

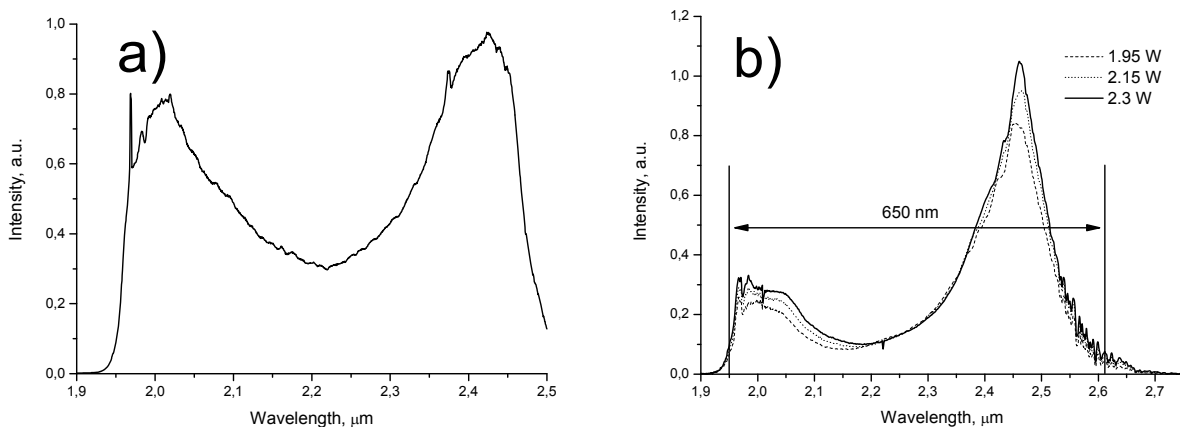


Figure 1. a) Typical output spectra a) of the Tm-doped fiber amplifier (5 W of output power) and b) of the fluoride fiber.

The main influence of the fluoride fiber on the input radiation spectrum is the redistribution of the power spectral density. Owing to the positive sign of the dispersion parameter, the solitonic components of the input spectrum experience a red-shift during propagation through the fiber. At some point, the red-shift is stopped due to the decrease of the Raman gain and increase of the glass host optical loss in the vicinity of the OH⁻ absorption (2.7 μm). As a result, we observe accumulation of the energy in the red part of the spectrum. The spectral peak gets narrower and the maximum is slightly shifted from 2.4 to 2.46 μm . The overall spectrum is broadened up to 650 nm at -10 dB level (1.95-2.6 μm), mostly due to the extension of the long-wavelength wing.

The germanate fibers with a solid splice to the amplifier experienced lower splice losses, allowing higher 2.5 and 2.15 W output power from the input powers of 4.65 and 4.3 W for the 6 cm 343 fiber and 6.5 cm 311 fiber, respectively. The

output spectra from both samples were quite similar (Fig. 2a). We suggest that the broadening and overall smoothing was due to the propagation in the negative-dispersion spectral region, but owing to strong nonlinearity the spectra were somewhat expanded in the blue direction as well. The resulting bandwidths at -10 level achieved 640 and 630 nm for 343 and 311 fibers, respectively. The spectrum of the 4-cm 357 fiber showed a narrower peak at about 2.5 μm resembling that of the fluoride fiber. We presumably this to be due to lower dispersion value for the 357 fiber. At -10 dB, the bandwidth reached 640 nm. The longer, 10.5 cm fiber sample produced spectrum broadening up to 830 (1.87-2.7 μm) and 1250 (1.66-2.91 μm) nm at -10 and -20 dB levels, respectively (Fig. 2b). The spectrum had much more complex structure, which we associate with the change of the dispersion sign at about 2.5 μm , as extrapolated from the data in¹¹. This fiber also had weaker absorption of the OH⁻ groups.

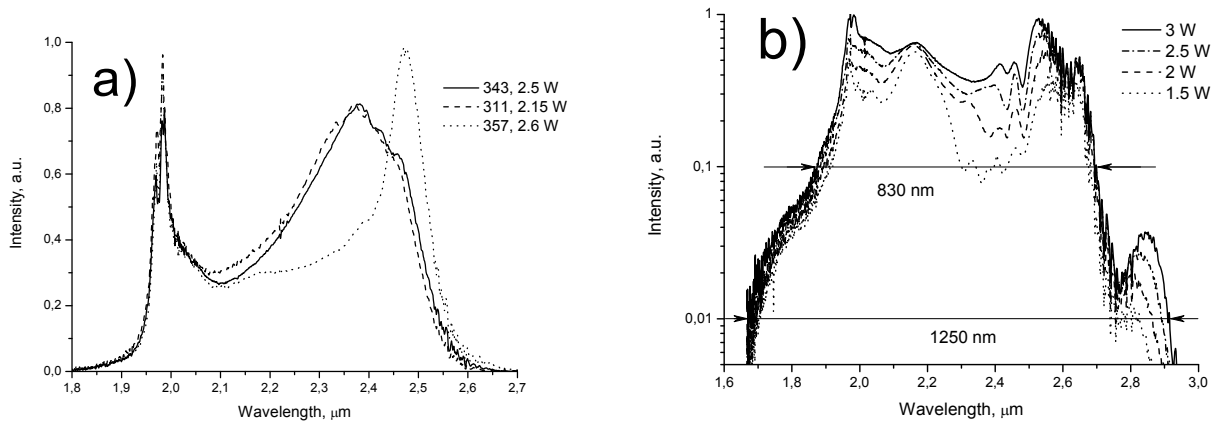


Fig. 2. Output spectra from the germanate fibers a) 343, 311 and 357 (4 cm) and b) 357 (10.5 cm).

The expanded spectrum allowed observation of the narrow atmospheric absorption lines (Fig. 3a), from the 1.65 m air propagation before entering the FTIR, and comparable propagation distance inside the device which was not isolated from the environment. The observed features correspond to atmospheric H₂O and CO₂ absorption¹².

Fig. 3b shows the dependence of the average output power on the pump power launched into the amplifier. For this fiber it was possible to achieve the SC power of 3.08 W. The optical-to-optical slope efficiency at high pump power of the laser system as a whole amounted to 13% for the 4-cm fiber and to 10% for the 10.5-cm sample.

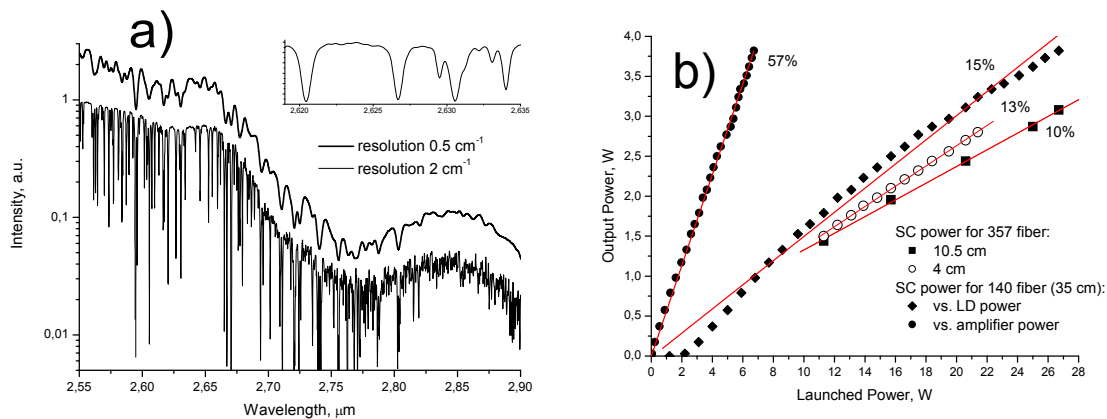


Fig. 3. Output spectrum of the 357 fiber (10.5 cm), an example of the fine structure is given in the inset (a), and the dependence of the output powers vs. launched into the amplifier pump power (b).

Even better results could be demonstrated with the last germanate fiber sample, where the output reached 3.82 W from 26.7 W of the launched pump power at 793 nm, corresponding to over 14% absolute and 15% average slope efficiency.

The efficiency decreased somewhat at higher pump powers because the expanded in the amplifier spectrum reached the high-loss spectral regions of the silica-based Tm-doped fiber⁸. Nevertheless, the 3.82 W of the output power corresponded to 57% of the power launched into the germanate fiber and efficiency curve is close to a linear dependence. The spectrum width reached 1250 nm at -10 dB level spanning from 1.93 to 3.18 μm . This result is unique for the oxide glasses with relatively large phonon energy. As in the previous case, the fine structure corresponding to the atmospheric absorption lines is visible in the spectrum (Fig. 4). The spectral band of the radiation fully covers the target spectral range from 2 to 3 μm . We believe that this result is not yet the limit, and expect further expansion of the generated supercontinuum into the mid-infrared.

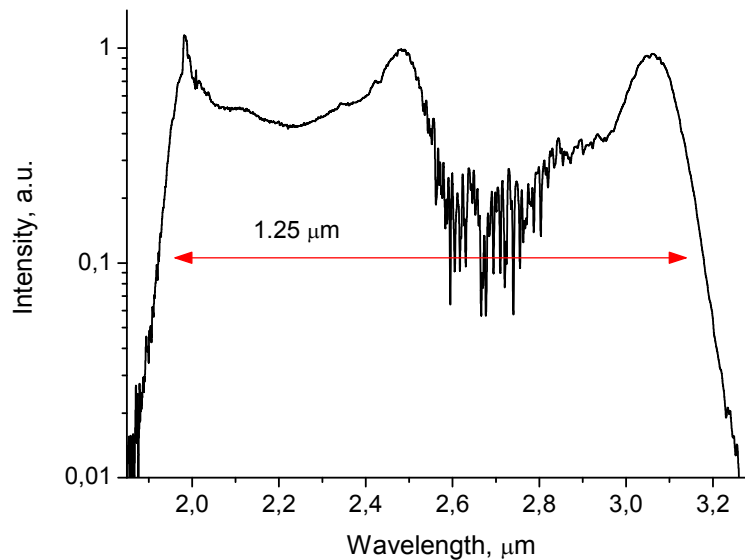


Fig. 4. Output spectrum of the supercontinuum generated in the pure germanate glass fiber.

CONCLUSIONS

We report generation of a high-power (up to 3.8 W), high-quality optical supercontinuum at 44 MHz pulse repetition rate in a germanate glass-core fibers covering the region of 1.87-2.7 μm (830 nm bandwidth) and 1.93-3.18 μm (1250 nm bandwidth) at -10 dB level. The all-fiber devices were built in MOPA configuration using a mode-locked Tm-doped fiber laser amplified in a Tm-doped fiber amplifier, with the nonlinear fiber directly spliced to the amplifier output.

Expansion of the supercontinuum spectrum beyond 3 μm in the oxide glass fiber is an exciting new result, opening up a huge potential for such fibers, which have the important advantage of being directly spliceable to the pulse source, thus enabling simple, robust and reliable devices.

The demonstrated setup produced a spectrum approaching the octave bandwidth and can be of an immediate interest for self-referenced frequency combs, trace gas sensing and environmental monitoring.

ACKNOWLEDGEMENTS

The work is supported by the NFR projects FRITEK/191614 and MARTEC project MLR.

REFERENCES

- [1] Y. Chen, E. Räikkönen, S. Kaasalainen, J. Suomalainen, T. Hakala, J. Hyypä, and R. Chen, "Two-channel hyperspectral LiDAR with a supercontinuum laser source," *Sensors (Basel)* 10, 7057-7066 (2010).
- [2] C. Courvoisier, A. Mussot, R. Bendoula, T. Sylvestre, J. G. Reyes, G. Tribillon, B. Wacogne, T. Gharbi, H. Maillotte, "Broadband supercontinuum in a microchip-laser-pumped conventional fiber: Toward biomedical applications," *Laser Phys.*, 507-514 (2004).
- [3] E. Sorokin "Ultrabroadband solid-state lasers in trace gas sensing," in *Mid-IR Coherent Sources and Applications*, Majid Ebrahim-Zadeh and Irina T. Sorokina (Springer, NATO science series II: Mathematics, Physics and Chemistry 2008) pp. 557-574.
- [4] A. S. Kurkov, V. A. Kamynin, E. M. Sholokhov, A. V. Marakulin, "Mid-IR supercontinuum generation in Ho-doped fiber amplifier," *Laser Phys. Lett.* 8, 754-757 (2011).
- [5] J. Geng, Q. Wang, and S. Jiang, "High-spectral-flatness mid-infrared supercontinuum generated from a Tm-doped fiber amplifier," *Applied Optics*, 51, 834-840 (2012).
- [6] J. Swiderski and M. Michalska, "Mid-infrared supercontinuum generation in a single-mode thulium-doped fiber amplifier," *Laser Phys. Lett.* 10, 035105 (2013).
- [7] J. Swiderski and M. Michalska, "The generation of a broadband, spectrally flat supercontinuum extended to the mid-infrared with the use of conventional passive single-mode fibers and thulium-doped single-mode fibers pumped by 1.55 μm pulses," *Laser Phys. Lett.* 10, 015106 (2013).
- [8] V.V. Dvoyrin and I. T. Sorokina, "5 W Supercontinuum Generation at 1.9-2.5 μm from a Tm-Doped All-Fiber MOPA Laser," in *Advanced Solid-State Lasers/Mid-Infrared Coherent Sources*, Technical Digest (CD) (Optical Society of America, 2013), paper MTh1C.3.
- [9] O.P. Kulkarni, V.V. Alexander, M. Kumar, M.J. Freeman, M.N. Islam, J.F.L. Terry, M. Neelakandan, and A. Chan, "Supercontinuum generation from ~ 1.9 to 4.5 μm in ZBLAN fiber with high average power generation beyond 3.8 μm using a thulium-doped fiber amplifier," *J. Opt. Soc. Am. B*, 28(10), 2486-2498, 2011.
- [10] D. Buccoliero, H. Steffensen, O. Bang, H. Ebendorff-Heidepriem, and T. M. Monro, "Thulium pumped high power supercontinuum in loss-determined optimum lengths of tellurite photonic crystal fiber," *Appl. Phys. Lett.*, 97, 061106 (2010).
- [11] D. Klimentov, N. Tolstik, V. Dvoyrin, V. Kalashnikov and I. Sorokina, "Broadband Dispersion Measurement of ZBLAN, Germanate and Silica Fibers in MidIR," *J. Lightwave Tech.* 30, 1943-1947 (2012).
- [12] L. S. Rothman, D. Jacquemart, A. Barbe, D. Chris Benner, M. Birk, L. R. Brown, M. R. Carleer, C. Chackerian Jr, K. Chance, L. H. Coudert, V. Dana, V. M. Devi, J. M. Flaud, R. R. Gamache, A. Goldman, J. M. Hartmann, K. W. Jucks, A. G. Maki, J. Y. Mandin, S. T. Massie, J. Orphal, A. Perrin, C. P. Rinsland, M. A. H. Smith, J. Tennyson, R. N. Tolchenov, R. A. Toth, J. Vander Auwera, P. Varanasi, G. Wagner, "The HITRAN 2004 molecular spectroscopic database," *J. Quant. Spectrosc. Radiat. Transfer* 96, 139-204 (2005).